Coherent atomic deflection by resonant standing waves

A. F. Bernhardt* and B. W. Shore
Lawrence Livermore National Laboratory, P. O. Box 5508, Livermore, California 94550
(Received 18 August 1980)

We extend the previous theoretical treatment of standing-wave deflection of two-level atoms to include nonresonant excitation, nonorthogonal laser and atomic beams, and excitation duration upper bounded only by atomic relaxation times. Numerically solving equations analogous to those of abruptly initiated multilevel atomic excitation, we find bounds on the maximum deflection fixed by balancing acquired kinetic energy against interaction energy. We find that frequency detuning or nonorthogonal orientation of laser and atomic beams can enhance the deflection and, given sufficiently long interaction time, one can observe deflections at larger discrete angles. We comment on the connection between these Bragg scatterings and multiphoton resonances.

I. INTRODUCTION

The advent of high-power tunable lasers has renewed interest in electromagnetic wave deflection of neutral atomic beams.[1] As previous work[2] has noted, irradiated atoms absorb and emit photons into the applied fields at an induced rate while occasionally emitting photons, in random directions, at the spontaneous rate. Beam deflection occurs when the atoms gain or lose momentum from the field.

The rate of momentum transfer depends upon the nature of the applied field. If the field consists of a single traveling wave, then the atoms gain momentum at the spontaneous emission rate: Each stimulated emission merely restores a photon to the field, whereas spontaneous emission creates a photon with randomly directed momentum to replace the absorbed photon. Thus the atoms gain, on average, one quantum of linear momentum with each spontaneous decay. Several authors have discussed this mechanism for deflecting atomic beams,[3] while others have reported demonstrations.[4]

Much faster rates of momentum transfer, and hence larger beam deflections, occur when the field comprises two or more traveling waves.[2] An atom can absorb a photon from one of the waves and be induced to emit into a different wave, thereby changing momentum at the induced emission rate. The greatest momentum transfer occurs when the absorbed and emitted photon are counterpropagating, i.e., the field is a standing wave. With laser fields the induced rate may exceed the spontaneous rate by many orders of magnitude, so that standing waves offer potential for more rapid and efficient beam deflection than do traveling waves. (Because the stimulated absorption and remission is coherent[5] it is the Rabi frequency rather than the Einstein or Milne B coefficient that fixes the induced rate—see below).

The deflection of atomic beams by resonant standing electromagnetic waves is analogous to the deflection of light by ultrasound.[6] The same equations also occur in treatments of stimulated Compton scattering of electrons and the free-electron laser.[7]

Hitherto the model[2] for coherent excitation and deflection of atomic beams by strong resonant standing electromagnetic waves has treated the quantized translational motion of a two-level atom in a classical monochromatic standing-wave field, with solutions to the resulting semiclassical time-dependent Schrodinger equation for the atomic motion restricted by the following constraints:

(i) The frequency of the field ω matches the Bohr transition frequency of the atom $E_A/\hbar$ (i.e. exact resonance).

(ii) The incident atomic beam is aligned perpendicular to the propagation axis of the waves.

(iii) The time duration of the atom-field interaction is sufficiently brief that the kinetic energy of deflection (i.e., energy from momentum transverse to the wave fronts) remains much smaller than the interaction energy, $\hbar\Omega$.

Within these limits one finds that during each Rabi period $1/\Omega$ the rms deflection momentum increases by $\hbar k/\sqrt{2}$, where $\hbar k = \hbar\omega/c$ is the photon momentum. The resulting rms momentum $\hbar k\Omega t/\sqrt{2}$ after time t contrasts strikingly with the value $\hbar k\sqrt{\Omega t}$ which one would predict on the basis of random walks, as occurs with rate-equation description of incoherent momentum transfer.[8]

The occurrence of coherence effects in deflection by standing waves makes an extension of previous work desirable in order to eliminate the foregoing restrictions. The present paper does this.

We examine the more general problem of atomic motion in a standing monochromatic wave, not necessarily resonant with the atomic transition frequency, with arbitrary orientation of laser and atomic beam axis, and with interaction times restricted only to be short compared with atomic

relaxation times. (For longer times relaxation processes destroy the coherence, and one must employ a rate-equation description of the momentum transfer.[8])

We idealize the field as having uniform amplitude within a sharply delineated volume, so that the moving atoms abruptly enter and leave a region of constant interaction strength. Thus our model sharply contrasts with adiabatic following models of excitation in which the interaction strength gradually increases.

We derive our Schrödinger equation (in Sec. II) by treating both the field amplitudes (for two counterpropagating waves) and the atomic motion quantum mechanically. This approach provides new insight into the mechanism responsible for resonant deflection by a standing wave: atomic absorption and emission transfer photons from one traveling wave to the counterpropagating wave, concomitantly altering the atomic momentum.

Although we approach the problem via quantized fields, we actually treat the strong-field limit: we neglect back reaction upon the fields by the atoms. The equations of motion are formally identical to equations previously studied for application of a sequentially linked N-level atom,[9-12] enabling us to apply both computational methods and physical insight developed in that context.

The nature of the solutions to the basic equations depend on the relative sizes of four energies: The energy detuning $\hbar\Delta$ of the laser frequency away from the Bohr frequency; the atom-field interaction energy $\hbar\Omega$; the initial component of atomic kinetic energy in the direction of laser propagation $p_0^2/2M$; and the photon-induced (deflection) kinetic energy. In the simplest case (Sec. VI below) the interaction energy greatly exceeds all other energies. The equations then have well-known analytic solutions in terms of Bessel functions.[2,10] Succeeding sections present consequences of significant deflection energy (long interaction times; Sec. IX), significant initial transverse momentum (Secs. X–XII) and significant frequency detuning (Sec. XIII).

For a resonantly tuned standing wave, oriented perpendicular to the atomic beam, we find that, although the deflection momentum initially increases linearly with time, this growth is limited: The deflection kinetic energy cannot greatly exceed $\hbar\Omega$. Once the deflection reaches this limit it begins to diminish. Over a long interaction time the deflection momentum becomes distributed over the range limited by the values $|p| \leq (2M\hbar\Omega)^{1/2}$. The probability of larger deflections falls exponentially with increasing $|p|$.

When initial transverse momentum p_0 is not negligible the maximum deflection is still bounded, but now positive and negative bounds differ. We show that one can enhance the beam deflection in one direction by appropriate nonorthogonal orientation of atom and laser beams.

For very large angles of incidence we observe Bragg scattering[7]: selected quantized angles for which deflection is very large. The expression for these angles is just the Bragg law[12] for scattering of (atomic) waves by periodic structure (the standing wave). We relate this Bragg scattering to multiphoton resonance phenomena of the N-level analog, in which n photons are coherently transferred from one traveling wave to the other.[7]

Shifting the field frequency away from resonance with the Bohr frequency enhances the effects of and opportunities for multiphoton resonances and hence permits much greater complexity in the deflection dynamics. We find that, as with nonorthogonal alignment, slight detuning can enhance the deflection.

II. THE HAMILTONIAN

We consider a collection of two-level atoms[13] moving under the influence of two near-resonant traveling-wave fields. The Hamiltonian for this system,

$$H = H_F + H_A + H_I \tag{2.1}$$

comprises the Hamiltonian for the free fields H_F, the Hamiltonian for a free-atom H_A (including both internal excitation and center-of-mass motion), and the interaction between fields and atom, H_I.

Let $\Phi_i(N_i)$ with $i = 1$ and 2, be photon number states describing waves with frequencies ω_i, propagation vectors $\vec{k}_i$, and photon numbers N_i; they are eigenstates of the free-field Hamiltonian H_F:

$$(H_F - N\hbar\omega_i)\Phi_i(N) = 0. \tag{2.2}$$

(We have here omitted the field zero-point energy.[14]) Let the atomic states $\psi_-(\vec{p})$ and $\psi_+(\vec{p})$ represent, respectively, the ground and excited states of a two-level atom governed by the free-atom Hamiltonian H_A:

$$\begin{aligned}(H_A - p^2/2M)\psi_-(p) &= 0,\\ (H_A - p^2/2M - E_A)\psi_+(\vec{p}) &= 0,\end{aligned} \tag{2.3}$$

where E_A is the excitation energy relative to the ground state, p is the atomic momentum, and M the atomic mass. (We neglect mass changes due to absorption and emission.)

For allowed transitions the dominant contribution to the interaction Hamiltonian comes from the electric-dipole interaction,

$$H_I = -\vec{\mu}\cdot\vec{E}. \tag{2.4}$$

In our derivation we shall take the electric field

to be the sum of two single modes of the radiation field which are either linearly polarized in the same direction or circularly polarized in opposite senses with respect to their propagation vectors. Following the derivation of the equations of motion we shall restrict ourselves to the case of counter-propagating waves ($\vec{k}_1 = -\vec{k}_2$). The field is assumed to have infinite extent in both the propagation direction, x, and one orthogonal direction, y. In the remaining direction, z, the field is characterized by a sudden turn on at $z = 0$, a constant amplitude for $0 < z < z_1$, and a sudden turn off at z_1. [It is a straightforward matter to construct a set of modes containing one mode with the desired spatial profile from the set $E_m = E_0 e^{ikx} \sin(m\pi z/z_1)$.]

Although we shall assume an electric-dipole interaction, our final equations and conclusions apply equally well to forbidden transitions: One need only replace the dipole transition moment by another electric or magnetic multipole moment.

III. BASIS STATES

To describe the system of atoms and fields we take basis states of the product form

$$\Phi_1(N_1)\,\Phi_2(N_2)\,\psi_\pm(\vec{p}). \tag{3.1}$$

Acting upon such a state the interaction Hamiltonian connects ψ_- with ψ_+, and vice versa, alters photon occupation numbers N_i by unity, and shifts atomic momentum $\vec{p}$ by increments of $\hbar\vec{k}$: We assume that the atom enters and leaves the interaction region very suddenly.

Consider as an initial-state one with well-defined photon number and an unexcited atom moving with momentum $\vec{p}$,

$$\Phi_0 = \phi_1(N_1)\,\phi_2(N_2)\,\psi_-(\vec{p}). \tag{3.2}$$

We consider the near-resonant condition

$$\hbar\omega_1 \cong \hbar\omega_2 \cong E_A. \tag{3.3}$$

Then resonant emission and absorption, conserving the energy $N_1\hbar\omega_1 + N_2\hbar\omega_2$, have much higher probabilities than do nonresonant processes. Therefore we confine our attention to transitions which approximately conserve energy and exactly conserve momentum. From this initial state the atom can absorb a photon from either of the two fields. Absorption of a photon from the first field reduces the occupation number N_1 by unity, promotes the atom from the ground to the excited state, and increases the atomic momentum by $\hbar\vec{k}_1$. This action produces the state

$$\Phi_1 = \phi_1(N_1 - 1)\phi_2(N_2)\psi_+(\vec{p} + \hbar\vec{k}_1). \tag{3.4}$$

Similarly absorption of a photon from the second field changes the state of the system to

$$\Phi_{-1} = \phi_1(N_1)\phi_2(N_2 - 1)\psi_+(\vec{p} + \hbar\vec{k}_2). \tag{3.5}$$

From the state Φ_1 either field can stimulate emission. If the atom emits a photon into field ϕ_1 the system returns to the initial-state ϕ_0. However, if it emits a photon into the second field ϕ_2 then the system progresses into the state

$$\Phi_2 = \phi_1(N_1 - 1)\phi_2(N_2 + 1)\psi_-(\vec{p} + \hbar\vec{k}_1 - h\vec{k}_2). \tag{3.6}$$

Similarly emission of a photon into field ϕ_1 from state Φ_{-1} generates the state

$$\Phi_{-2} = \phi_1(N_1 + 1)\phi_2(N_2 - 1)\psi_-(\vec{p} - \hbar\vec{k}_1 + \hbar\vec{k}_2). \tag{3.7}$$

Generalizing this analysis we see that stimulated emission and absorption carries the system through a succession of momentum and energy conserving states having the form

$$\Phi_n(\vec{p}) = \phi_1\left(N_1 - \frac{n}{2}\right)\phi_2\left(N_2 + \frac{n}{2}\right)\psi_-\left(\vec{p} + \frac{n}{2}\hbar\vec{k}_1 - \frac{n}{2}\hbar\vec{k}_2\right) \tag{3.8}$$

for n an even integer, or

$$\Phi_n(\vec{p}) = \phi_1\left(N_1 - \frac{n+1}{2}\right)\phi_2\left(N_2 + \frac{n-1}{2}\right) \times \psi_+\left(\vec{p} + \frac{n+1}{2}\hbar\vec{k}_1 - \frac{n-1}{2}\hbar\vec{k}_2\right) \tag{3.9}$$

for n an odd integer.

Figure 1 illustrates the linked changes in fields

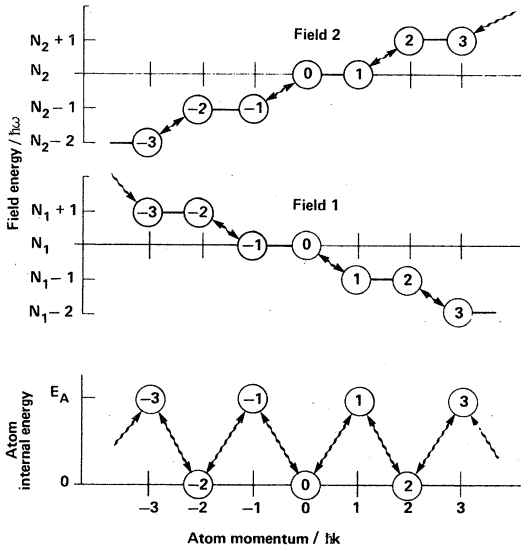

FIG. 1. Basis states of combined atom-field system. Abscissa expresses atomic momentum in units of photon momentum $\hbar k$, ordinate expresses excitation energy of field 2 (uppermost curve), field 1 (middle curve), and atom (lowest curve). Arrows show allowed linkages between basis states (encircled numbers are the index n labeling basis state Φ_n).

and atom encompassed by these basis states, for the particular case of exact resonance ($\hbar\omega_1 = \hbar\omega_2 = E_A$), and counter-propagating beams ($\vec{k}_2 = -\vec{k}_1$): the transfer of photons from field 1 to field 2 accompanies a change of atomic momentum. Note that the basis-state index n (shown encircled) also measures the alteration in atomic momentum $n\hbar\vec{k}$.

IV. THE SCHRÖDINGER EQUATION

By restricting consideration to time intervals which are shorter than the natural lifetime of the excited state we can neglect spontaneous emission. Then the system state vector $\Psi(t)$ remains within the space spanned by the basis states Φ_n, and we can write

$$\Psi(t) = \int d\vec{p} \sum C_n(\vec{p}, t)\Phi_n(\vec{p})\exp(-i\alpha_n t). \tag{4.1}$$

We are at liberty to choose the phases α_n for subsequent mathematical convenience; we discuss our phase convention below. In this basis state the diagonal elements of the Hamiltonian are

$$\langle\Phi_n(\vec{p})|H|\Phi_n(\vec{p}')\rangle = \langle\Phi_n|H_A + H_F|\Phi_n\rangle \equiv H_{nn}$$

$$H_{nn} = \begin{cases} \left[\left(N_1 - \frac{n}{2}\right)\hbar\omega_1 + \left(N_2 + \frac{n}{2}\right)\hbar\omega_2 + \frac{1}{2M}\left(\vec{p} + \frac{n}{2}\hbar\vec{k}_1 - \frac{n}{2}\hbar\vec{k}_2\right)^2\right]\vec{\delta}(\vec{p}' - \vec{p}), & n \text{ even} \\ \left[\left(N_1 - \frac{n+1}{2}\right)\hbar\omega_1 + \left(N_2 + \frac{n-1}{2}\right)\hbar\omega_2 + E_A + \frac{1}{2M}\left(\vec{p} + \frac{n+1}{2}\hbar\vec{k}_1 - \frac{n-1}{2}\hbar\vec{k}_2\right)^2\right]\vec{\delta}(\vec{p}' - \vec{p}), & n \text{ odd} \end{cases} \tag{4.2}$$

where the Dirac brackets indicate integration over electronic coordinates, and center-of-mass coordinates. The nonvanishing off-diagonal elements are

$$\langle\Phi_{n+1}(\vec{p})|H|\Phi_n(\vec{p}')\rangle = H_{n+1,n}$$

$$H_{n+1} = \begin{cases} -\left[\frac{\hbar\omega_1}{2V}\left(N_1 - \frac{n}{2}\right)\right]^{1/2}\mu\frac{\sin(p_z' - p_z)z_1/\hbar}{p_z' - p_z}\delta(p_x' - p_x + \hbar k_1)\,\delta(p_y' - p_y), & n \text{ even} \\ -\left[\frac{\hbar\omega_2}{2V}\left(N_2 + \frac{n+1}{2}\right)\right]^{1/2}\mu\frac{\sin(p_z' - p_z)z_1/\hbar}{p_z' - p_z}\delta(p_x' - p_x - \hbar k_2)\delta(p_y' - p_y), & n \text{ odd} \end{cases} \tag{4.3}$$

where μ is the component of the dipole transition moment along the E-field polarization direction. (We have taken μ to be real and positive, a choice always possible by suitable choice of internal atomic basis phases.)

In this basis the Hamiltonian matrix is tridiagonal. The matrix has dimension $N_1 + N_2$ because, in principle, all photons can be transferred from the first field to the second, and vice versa. Our interest centers on those basis states Φ_n for which n is far from these extreme values, so that we shall neglect the n dependence of the off-diagonal elements.

When the expansion (4.1), is substituted into the time-dependent Schrödinger equation, and the integration over momentum is carried out, we find the following set of coupled ordinary differential equations for the probability amplitudes $C_n \equiv C_n(\vec{p}, t)$:

$$\begin{aligned} i\hbar\frac{d}{dt}C_n &= (H_{nn} - \hbar\alpha_n)C_n + H_{n,n-1}e^{-i(\alpha_n - \alpha_{n-1})t}C_{n-1} \\ &\quad + H_{n;n+1}e^{-i(\alpha_n - \alpha_{n+1})t}C_{n+1} \\ &\equiv \sum \hbar W_{nm}C_m. \end{aligned} \tag{4.4}$$

Note that the equations of motion assume this simple form because of our choice of spacial profile of the field. If we choose a Gaussian spacial profile, for example, we obtain the Eqs. (4.4) only in the case where the C_n can be assumed to be slowly varying functions of p_z compared to the Fourier transform of the Gaussian spacial profile. At this point we can choose the phases α_n to eliminate, as far as possible, the time dependence of the coefficient matrix W, as expressed through exponential terms. We make the choice

$$\hbar\alpha_n = \left(N_1 - \frac{n}{2}\right)\hbar\omega_1 + \left(N_2 + \frac{n}{2}\right)\hbar\omega_2 + \tfrac{1}{2}(E_A - \hbar\omega_2) + E_0, \tag{4.5a}$$

for n even, and

$$\hbar\alpha_n = \left(N_1 - \frac{n+1}{2}\right)\hbar\omega_1 + \left(N_2 + \frac{n-1}{2}\right)\hbar\omega_2 + \tfrac{1}{2}(E_A - \hbar\omega_1) + E_0, \tag{4.5b}$$

for n odd. Here E_0 is an arbitrary reference energy. With this choice of phases the Schrodinger equation becomes

$$i\hbar\frac{d}{dt}C_n = C_n\begin{cases}\frac{1}{2M}\left(\vec{p}+\frac{n}{2}\hbar\vec{k}_1-\frac{n}{2}\hbar\vec{k}_2\right)^2-\frac{1}{2}(E_A-\hbar\omega_2)-E_0, & \text{even } n\\ \frac{1}{2M}\left(\vec{p}+\frac{n+1}{2}\hbar\vec{k}_1-\frac{n-1}{2}\hbar\vec{k}_2\right)^2+\frac{1}{2}(E_A-\hbar\omega_1)-E_0, & \text{odd } n\end{cases} \tag{4.6}$$
$$-C_{n-1}\frac{\hbar\Omega_1}{2}e^{-i(\omega_2-\omega_1)t/2}-C_{n+1}\frac{\hbar\Omega_2}{2}e^{+i(\omega_2-\omega_1)t/2},$$

where ω_i is the Rabi frequency

$$\hbar\Omega_i = \mu(N_i\hbar\omega_i/2V)^{1/2}. \tag{4.7}$$

These equations of motion simplify greatly when we consider the case of equal frequency ($\omega_1=\omega_2$) oppositely directed ($\vec{k}_2=-\vec{k}_1$) fields of equal intensity ($N_1=N_2$). The initial atomic momentum $\vec{p}$ has a component p_0 which parallels the counterpropagating beam axis (i.e., which is *transverse* to the standing wave fronts), and a much larger component p_1 perpendicular to the laser beams. This latter component is unaffected by the stimulated emission and absorption processes; it provides a constant atomic velocity across the laser beam. We can remove this component of kinetic energy by setting

$$E_0=\frac{1}{2M}(p_1)^2+\frac{1}{2M}(p_0)^2\equiv\frac{p^2}{2M}. \tag{4.8}$$

Then the equations can finally be written as

$$i\frac{d}{dt}C_n=\left(b(2qn+n^2)\pm\frac{\Delta}{2}\right)C_n-\frac{\Omega}{2}(C_{n-1}+C_{n+1}). \tag{4.9}$$

Here the + (−) sign refers to even (odd) n; the term Δ is the off-resonant detuning

$$\hbar\Delta\equiv E_A-\hbar\omega_1=E_A-\hbar\omega_2, \tag{4.10}$$

and we have introduced the parameters

$$b\equiv\hbar k^2/2M,\quad q\equiv p_0/\hbar k. \tag{4.11}$$

V. SEMICLASSICAL DERIVATION

Although our derivation of Eq. (4.9) proceeded from a quantized amplitude representation of the fields, thereby facilitating a photon picture of momentum exchange between fields and atom, the resulting equation of motion can be obtained by extending the previous semiclassical approach.[2] We take as our basis states the atomic states

$$\Phi_n=\psi_\pm(p_0+n\hbar k), \tag{5.1}$$

and choose our phases to be

$$\hbar\alpha_n=E_0\pm\tfrac{1}{2}\hbar\Delta, \tag{5.2}$$

where the upper (lower) sign refers to even (odd) n. In place of the quantized electric field we have the semiclassical expression

$$H_I=2\hbar\Omega\cos(\omega t)\cos(\vec{k}\cdot\vec{r}). \tag{5.3}$$

Upon evaluating matrix elements of $H=H_A+H_I$ in this basis and neglecting rapidly varying terms $e^{\pm 2i\omega t}$ compared with unity (the rotating-wave approximation[9]) we recover Eq. (4.9).

VI. THE N-LEVEL ANALOG

Equation (4.9) is identical with that which one obtains for a sequentially linked multilevel system interacting with classical monochromatic electric fields in the rotating-wave approximation—a model sometimes dubbed the N-level atom.[9-11] In the latter model, as in our atomic-beam deflection, the off-diagonal elements of the matrix $\hbar W$ are interaction energies, the diagonal elements W_{nn} are cumulative detunings.

In the multilevel system of Eq. (4.9) each transition has equal interaction energy—the "equal Rabi" case. The detuning has two distinct terms:

(i) An alternating term $\pm\Delta/2$ expressing frequency detuning away from the Bohr transition frequency $E_A/\hbar$;

(ii) A kinetic-energy detuning $b(2qn+n^2)$ comprising a photon-induced detuning $bn^2=n^2\hbar k^2/2M$ and a cross term $2bqn=p_0nk/M$ which is n times the single-photon Doppler shift.

Because the kinetic detuning grows quadratically with excitation level n it is analogous to the (frequency) detuning which occurs with an N-level model of an anharmonic oscillator. Note, however, that unlike the traditional treatments of an N-level atom or molecule, where energy levels bear positive integer labels $n=0, 1, 2, \ldots, N$, our model deals with the sequence of negative and positive integers $n=\ldots, -2, -1, 0, +1, +2, \ldots$. That is, our initial state corresponds to a highly excited state of the N-level system. Although our tridiagonal matrix has dimension bounded by photon occupation number, $-N<n<N$, the equal-Rabi form (4.9) holds only for $|n|\ll N$: When n becomes comparable to N we must return to Eq. (4.3) for the n dependence of Ω.

VII. DEFLECTION ANGLES

From solutions to Eq. (4.9) one computes the probability $P_n(t)=|C_n(t)|^2$ of finding that an atom

has acquired transverse momentum $n\hbar k$ at time t. Initially the atom had transverse momentum p_0 and moved at an angle of incidence Θ_0 with respect to the wave fronts (the xz plane)

$$\tan\Theta_0 = p_0/p_1 \quad \text{or} \quad \sin\Theta_0 = p_0/p. \tag{7.1}$$

Here $p = (p_1^2 + p_0^2)^{1/2}$ is the initial atomic momentum. The absorption of n photons changes the transverse momentum to $p_0 + n\hbar k$ and increments the angle Θ_0 by Θ, the deflection away from the initial direction. (See Fig. 2). Because p_1 is unaffected by the field, we have the relationship

$$\tan(\Theta_0 + \Theta) = (p_0 + n\hbar k)/p_1 \tag{7.2}$$

for the deflection. When $p_0 = 0$ (i.e., $\Theta_0 = 0$) the deflection relationship reads simply

$$\sin\theta = n\hbar k/p. \tag{7.3}$$

Readily measurable deflections typically occur with n values of several hundred.

The nature of the solutions to the basic equations (4.9) depends upon the relative size of four frequencies: the laser off-resonance detuning Δ; the Rabi frequency Ω; the initial transverse kinetic-energy detuning $bq^2 \equiv p_0/2Mk$; and the photon-induced (deflection) kinetic detuning bn^2. In the following section we examine the case where Ω is much larger than any other frequency. In subsequent sections we examine successively cases where bn^2, bq^2, and finally Δ play important roles in the dynamics.

The solutions also depend upon the initial conditions. We shall generally assume that at time $t = 0$, all population resides in level $n = 0$.

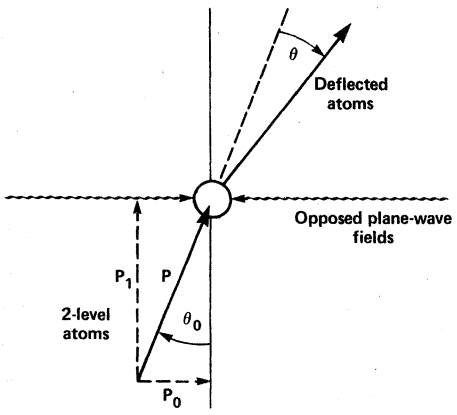

FIG. 2. Geometry of beam deflection. Initial atomic momentum $\vec{p}$ is resolved into components p_1 and p_0, respectively, normal to and along laser axis. After interaction the deflection away from incident direction is Θ.

VIII. ANALYTIC SOLUTIONS: NO DETUNING

The simplest soluble case of Eq. (4.9) occurs when the detuning is much less than the Rabi frequency

$$|b(2qn + n^2) \pm \frac{\Delta}{2}| \ll \frac{\Omega}{2}. \tag{8.1}$$

Under this restriction,[2,10] the equation reduces to

$$i\frac{d}{dt}C_n = -\frac{\Omega}{2}(C_{n-1} + C_{n+1}), \tag{8.2}$$

which has solutions expressible as cylinder functions. The solution of interest to us must have unit magnitude at $t = 0$, and so, apart from an arbitrary phase common to all C_n, it is i^n times the Bessel function of order n:

$$C_n(t) = i^n J_n(\Omega t). \tag{8.3}$$

Here the label $n = 0$ identifies the state in which all population resides when $t = 0$.

The Bessel-function probability distribution for multilevel excitation in the absence of detuning is well known:

$$P_n(t) = J_n^2(\Omega t). \tag{8.4}$$

Here we interpret $P_n(t)$ as the probability that the atom has at time t acquired momentum $n\hbar k$ along the laser beams by transferring photons from one field to the other field. Because the Bessel function has the symmetry

$$J_{-n}(x) = (-1)^n J_n(x), \tag{8.5}$$

we find equal probabilities for momentum $+n\hbar k$ and $-n\hbar k$:

$$P_{-n}(t) = P_n(t). \tag{8.6}$$

As previous articles have noted,[2,7,10] the Bessel function population flow follows a dominantly double-peaked pattern, symmetrically distributed about the initial-state $n = 0$. As the system evolves in time, population reaches and then passes by levels with increasingly large values of $|n|$. There is never appreciable population in levels much beyond the leading edge of the probability distribution, levels for which the order of the Bessel function equals its argument, $n = \Omega t$. A first burst of probability arrives at level n at roughly the time

$$t_b \cong n/\Omega, \tag{8.7}$$

after which the probability undergoes damped oscillations.

The Bessel-function approximation remains valid so long as one can neglect detuning compared with the Rabi frequency. Even if $\Delta = 0$ and $q = 0$, population will arrive in due time in levels for which bn^2 no longer remains negligible compared

with Ω, and the approximation 8.1 then fails. The following section discusses this failure.

IX. NO DETUNING, LONG INTERACTION TIMES

The next simplest case occurs when we assume resonantly tuned lasers, $\Delta = 0$, and an atomic beam moving parallel to the standing wave fronts of the lasers, $p_0 = 0$, but we no longer impose the restriction $bn^2 \ll \Omega$. Such atoms have deflection amplitudes governed by the equation

$$i\frac{d}{dt}C_n = bn^2 C_n - \frac{\Omega}{2}(C_{n-1} + C_{n+1}). \tag{9.1}$$

The simple change of variables

$$C_n(t) = (i)^n R_n\left(\frac{p}{\Omega} : x - \Omega t\right), \tag{9.2}$$

where $p = b/\Omega$ and $x = \Omega t$, converts this equation into the Raman-Nath equation[6]

$$2\frac{d}{dx}R_n = \rho n^2 R_n + R_{n-1} - R_{n+1} \tag{9.3}$$

for the Raman-Nath functions $R_n(\rho; x)$ (our terminology) whose properties have been examined for application to the diffraction of light by ultrasound waves in a dielectric liquid.[6]

It is instructive to examine a relief view of the probability distribution $P_n(t)$ as a function of n and time. Figure 3 displays such a view, obtained by numerical solution of Eq. (8.1) for the parameter choices $\Omega = 1$, $b = 0.05$. In this picture one observes two peaks of probability moving away from $n = 0$ at the rates $\pm\Omega t$, in accord with the Bessel-function approximation. This pattern of probability flow ceases on reaching the turning-point levels where detuning equals the Rabi frequency:

$$|n_{max}| \cong \sqrt{\Omega/b}\,. \tag{9.4}$$

For the present example this formula gives $|n_{max}| = 4.5$. The time of this failure of the Bessel-function approximation is roughly $t_f = |n_{max}|/\Omega \cong 5$. At longer times the probability distribution undergoes more complicated variations, but remains almost entirely within bounds $\pm|n_{max}|$.

For levels beyond the range $|n| > n_{max}$ the population falls exponentially with increasing n. Thus in practice one can treat a truncated system of equations without introducing appreciable error. For the examples in this paper we used 31 levels.

Equation (9.1), the equal-Rabi system with quadratic detuning, describes the dynamics of an anharmonic oscillator initially in a highly excited state n_0: The index n expresses the deviation away from this initial state. (We neglect the n variation in the oscillator dipole moment, proportional to $n_0 + n$, just as we have approximated $N + n$ by N in the Rabi frequency for our beam deflection.) Although such an anharmonic oscillator is not strictly periodic, a significant portion of the probability does return to the initial state $n = 0$ after a period of time. Figure 3 shows quite clearly this peak in p_0.

In interpreting the time-dependent dynamics displayed in Fig. 3 it is useful to think of the probability $P_n(t)$ as a fluid which, following initial release from confinement at $n = 0$, flows as a wave packet toward larger $|n|$ until it reflects from a soft barrier at $|n_{max}|$. The probability then sloshes back toward $n = 0$ where it subsequently piles up and then again spreads out.

Although the Bessel-function approximation predicts deflections which increase linearly with exposure time (and hence linearly with thickness of the laser interaction zone), kinetic detuning limits deflections to a maximum

$$\Theta_{max} = \arctan\left(\frac{n_{max}\hbar k}{p_1}\right). \tag{9.5}$$

As we see from Fig. 3, there is an optimum time (thickness) for which this deflection occurs; it is the time t_f. Longer exposure times may actually diminish the deflection. Over extremely long times the deflection will be diluted over a range of angles less than Θ_{max}.

Note that, so long as diagonal elements of the Hamiltonian remain negligible compared with Ω, one can admit a time varying interaction without altering the qualitative pattern of excitation: one introduces an interaction duration

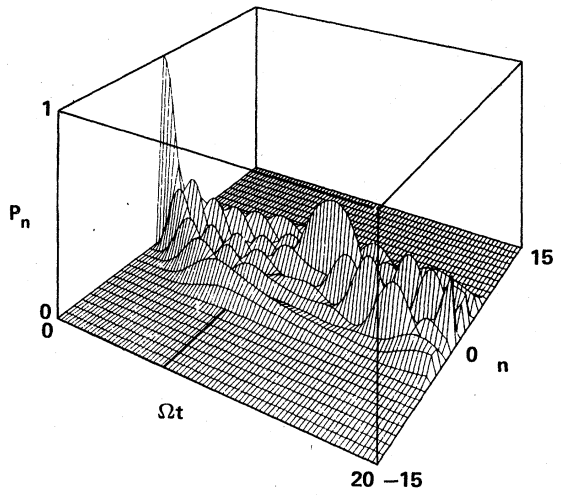

FIG. 3. Relief view of probability distribution $p_n(t)$ as a function of n and Ωt.

$$X(t) = \int dt' \Omega(t'), \quad dX = dt\,\Omega(t), \tag{9.6}$$

so that Eq. 8.2 becomes

$$-i2\frac{d}{dX}C_n = C_{n-1} + C_{n+1}, \tag{9.7}$$

with the solution

$$C_n(t) = i^n J_n(X(t)). \tag{9.8}$$

This result means that, within the Bessel approximation, the atom can enter (or leave) the field gradually without altering the analytic form of the probability distribution. Thus we see that our assumed abrupt initiation of atom-field interaction at a sharp boundary only requires that the field intensity reach full value before the deflection departs significantly from that predicted by Bessel-function approximation.

X. NONORTHOGONAL LASER AND ATOM BEAMS

We have seen that when the atomic beam crosses the laser beam at right angles, the atomic beam diffracts into a pattern symmetric about the incident atomic-beam axis (see Fig. 4). The population flow arrives simultaneously into two turning-point levels $+n_{max}$ and $-n_{max}$, corresponding to maximum deflection angles $\pm\Theta_m$ where

$$\Theta_m = \arctan(|n_{max}|\hbar k/p_1). \tag{10.1}$$

When the atomic beam approaches the laser beam at some nonzero angle of incidence $\Theta_0 = \sin^{-1}(p_0/p)$ (measured clockwise from a normal to the photon axis—see Fig. 4) then the deflection pattern becomes more complicated. For sufficiently short interaction times the pattern is symmetric about the incident atomic-beam axis. However, population turning-points levels are no longer symmetric about $n = 0$: for positive p_0 the population flow first encounters a turning point at positive n, say n_1, and subsequently reaches a turning point for negative n, say, n_2. This means that there are now two distinct maximum deflection angles: A negative deflection

$$\Theta_2 = \arctan[(p_0 + n_2\hbar k)/p_1] - \arctan(p_0/p_1), \tag{10.2}$$

which is greater in magnitude than Θ_m, and a positive deflection

$$\Theta_1 = \arctan[(p_0 + n_1\hbar k)/p_1] - \arctan(p_0/p_1), \tag{10.3}$$

which is smaller than Θ_m; see Fig. 4. Thus one enhances the maximum achievable deflection by aligning atom and photon beams at an angle. (Below we discuss limitations imposed upon Θ_0 and the optimum value of Θ_0.) Note that the maximum deflection angles remain symmetric about the plane normal to the photon propagation axis.)

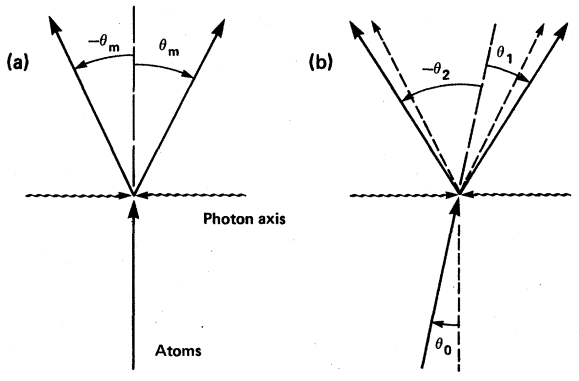

FIG. 4. Maximum delfection angles. (a): Angles $\pm\Theta_m$ for incident atomic beam normal to photon axis. (b): Maximum deflection Angles Θ_1 and Θ_2 for initial atomic beam oriented at angle Θ_0 with respect to normal direction of photon axis.

Figure 5 illustrates the probability distributions as a function of interaction time for several choices of incident angle. Each frame depicts the probability $P_n(t)$, as in Fig. 3, for a specific integer choice of the parameter $m = p_0/\hbar k$. We observe, in the frames for $|m| = 3$ and 6, that the deflection pattern becomes asymmetric about $n = 0$, following a brief interval during which the Bessel-function approximation applies. When $m > 0$ the population favors $n < 0$ whereas $m < 0$ favors $n > 0$. That is, the beam is bent back on itself. We see that $m = 6$ permits much larger n values than does $|m| = 3$: increasing the angle of incidence has increased the deflection. As we consider the still larger $|m|$ values, $|m| = 9$, we see that the probability distribution has become confined to a narrow band around the initial value $n = 0$: There is little deflection of the incident beam. Thus we see that there exists an optimum orientation angle and time to maximize deflection.

It is not difficult to find explanations for this behavior of the N-level model for atomic deflection. Suppose that the beam of resonantly excited ($n = 0$) atoms approaches the standing wave at some finite angle θ_0, say the deflection angle which would be obtained by the absorption of the momentum from m photons. Then the initial value of the transverse atomic momentum is $p_0 = m\hbar k$ and the equation of motion reads

$$i\frac{d}{dt}C_n = b(m+n)^2 C_n - \frac{\Omega}{2}(C_{n-1} + C_{n+1}). \tag{10.4}$$

(Here we have taken $E_0 = p_1^2/2M$.) We observe that this equation obtains for the case $p_0 = 0$ but with an expansion with shifted indices.

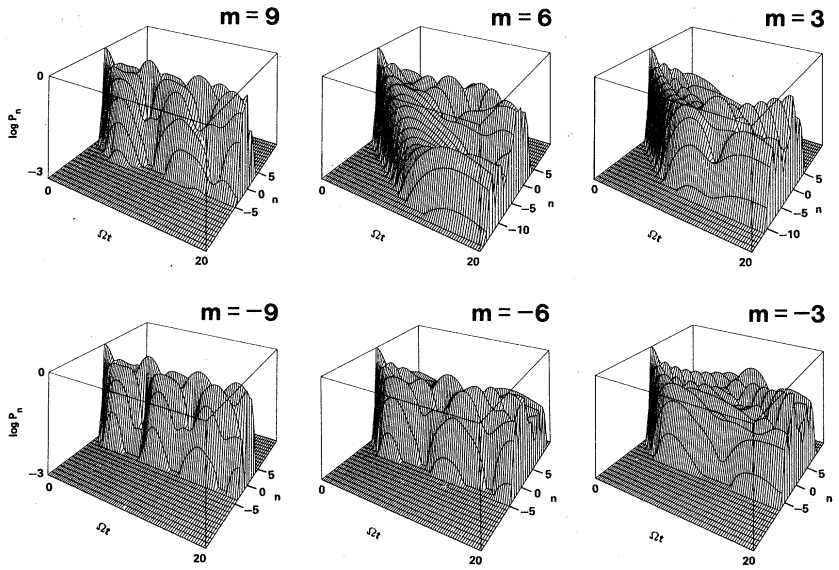

FIG. 5. Relief view of $\log P_n(t)$ as a function of n and Ωt for selected values of the initial transverse momentum $p_0 = m\hbar k$ with, in clockwise order, $m = 9$, 6, 3, -3, -6, and -9. Other details are as in Fig. 3.

$$\Psi(t) = \begin{cases} \sum C_n(t)\,\Phi_{n+m}\,e^{-i\alpha_{n+m}t}, \\ \sum C_{n-m}(t)\,\Phi_n\,e^{-i\alpha_n t}. \end{cases} \tag{10.5}$$

Thus our amplitudes $C_n(t)$ are still expressible as Raman-Nath functions, but now we require the initial condition

$$|C_n(0)| = \delta_{n,m}. \tag{10.6}$$

That is, we deal with population initially in level m rather than level 0.

As long as the detuning term remains much smaller than the Rabi term we have the Bessel-function approximation

$$C_n(t) = i^{n+m} J_{n+m}(\Omega t). \tag{10.7}$$

This approximation holds for times

$$n < \left(\frac{\Omega}{b} + m^2\right)^{1/2} - m \tag{10.8}$$

However, if m is sufficiently large the inequality 10.8 cannot be satisfied except at $n = 0$; the Bessel-function approximation never applies. Indeed, if we are in the regime for which kinetic energy dominates interaction energies,

$$\frac{p_0^2}{2M} \gg \frac{\hbar\Omega}{2} \quad \text{or} \quad bq^2 \gg \frac{\Omega}{2}, \tag{10.9}$$

then our equation becomes approximately

$$i\frac{d}{dt}C_n = \frac{p_0^2}{2M\hbar}C_n, \tag{10.10}$$

with the solution

$$C_n(t) = \exp[i(p_0^2/2M\hbar)t]C_n(0). \tag{10.11}$$

Thus the probability remains fixed in time, locked into the initially populated level; there is no deflection, except for Bragg scattering (see below).

XI. GRAPHICAL INTERPRETATION

A few simple rules prove helpful in unifying the trends of probability distribution observed in these and other examples. One observes that population tends to accumulate in n values where the interaction energy greatly exceeds the kinetic and detuning energies, and that very little population ever reaches levels for which the interaction energy is much smaller than the kinetic and detuning energies.

We can quantify this observation by comparing the magnitude of the diagonal elements of the Hamiltonian

$$f(n) \equiv |W_{nn}| = \left|b(2qn + n^2) \pm \frac{\Delta}{2}\right|, \tag{11.1}$$

with the magnitude of the Rabi frequency Ω. We have chosen the zero-point energy E_0 such that $f(n)$ vanishes when n is the initial level. Then one finds that the long-time average population[11]

$$\bar{P}_n = \lim_{T\to\infty} \frac{1}{T}\int_0^T dt\, P_n(t) \tag{11.2}$$

accumulates in n values for which $f(n) \ll |\Omega|$ and avoids n values for which $f(n) \gg |\Omega|$. The "turning point" of probability flow occurs when $f(n) = |\Omega|$.

Figure 6 plots examples of $f(n)$, the (constant) value of $|\Omega|$ and, on a logarithmic scale, the cor-

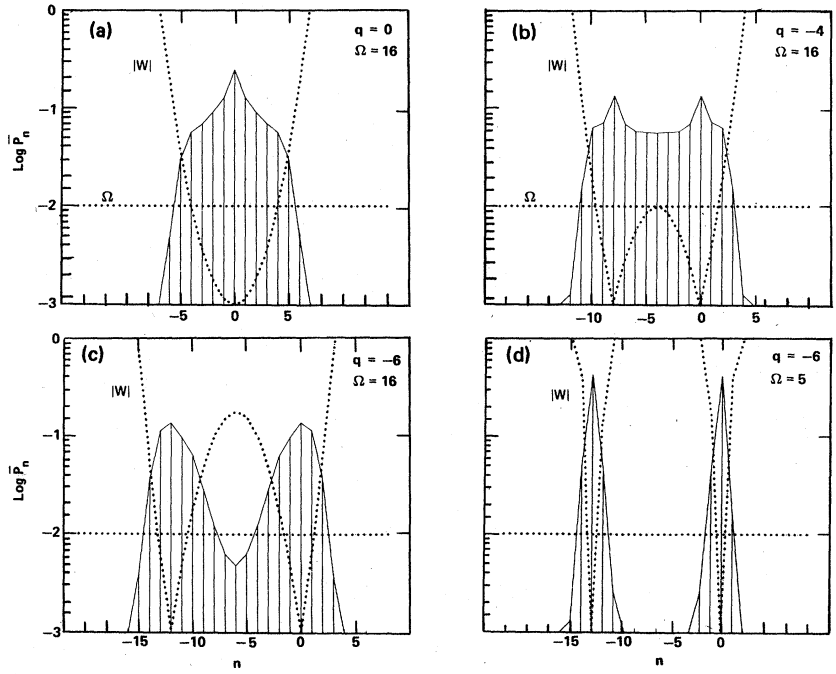

FIG. 6. Full lines show plots of the long-time average probability P_n versus n on a logarithmic scale, for on-resonant tuning. Dotted lines show values of magnitudes of diagonal elements $|W_{nn}|$ and $|\Omega_n|$ on a linear scale. (a): $q=0$, $\Omega=16$, (b): $q=-4$, $\Omega=16$, (c): $q=-6$, $\Omega=16$; (d): $q=-q$, $\Omega=5$.

responding values of $\bar{P}_n$. With resonant tuning ($\Delta=0$) and orthogonal laser-atom beams ($q=0$), the function $f(n)$ is a parabola and the probability is confined to a symmetric region around the initial value $n=0$: see Fig. 6(a). The value $n=0$ dominates the probability distribution.

When the atomic-beam angle of incidence is nonzero the parabola tilts; the absolute value sign produces a broad central peak of $f(n)$, and population tends to avoid $n=0$ while accumulating in two symmetrically placed values of n; see Fig. 6(b). So long as $|\Omega|$ greatly exceeds the height of the central peak, which is $f(-q)=bq^2$, the effect of nonzero $q=p_0/\hbar k$ is to broaden the region of likely n values and hence to enhance the deflection. However, if Ω is much smaller than bq^2, then there are two unconnected intervals of n values in which the probability accumulates, centered about $n=0$ and $n=-q$. See Fig. 6(c). Only if the second of these intervals encompasses an integer will population be found in any level but the initial one, $n=0$. Fig. 6(d) shows an example of this type.

XII. BRAGG RESONANCES

Although the population at first remains confined to the allowed region contiguous with the initially populated level $n=0$, after sufficient time the population can "tunnel" through the forbidden region, bypassing the virtual levels for which $n^2+2nq>\Omega/b$. By so doing, the population can, in due time, reach levels within a width $(\Omega/b+q^2)^{1/2}-q$ around the value $2q$. This population oscillation is an illustration of what, for the N-level atom, would be termed a *multiphoton resonance*. Here, whenever $q\equiv p_0/\hbar k$ is an integer or half-

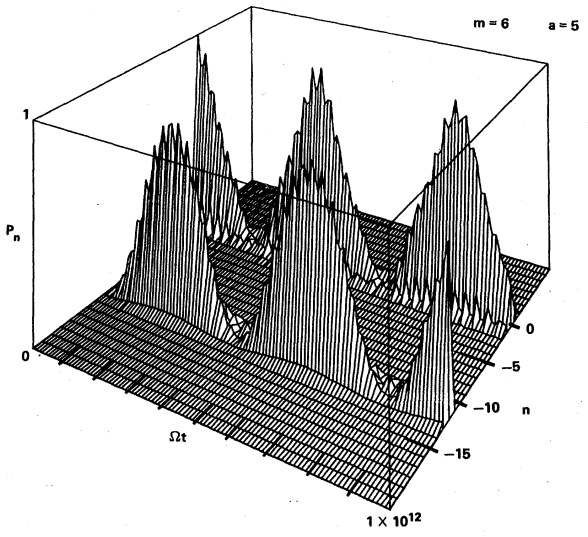

FIG. 7. Log P_n as a function of n and Ωt. For sufficiently long times, population tunnels from one energy-conserving set of n values to the other. This is Bragg scattering.

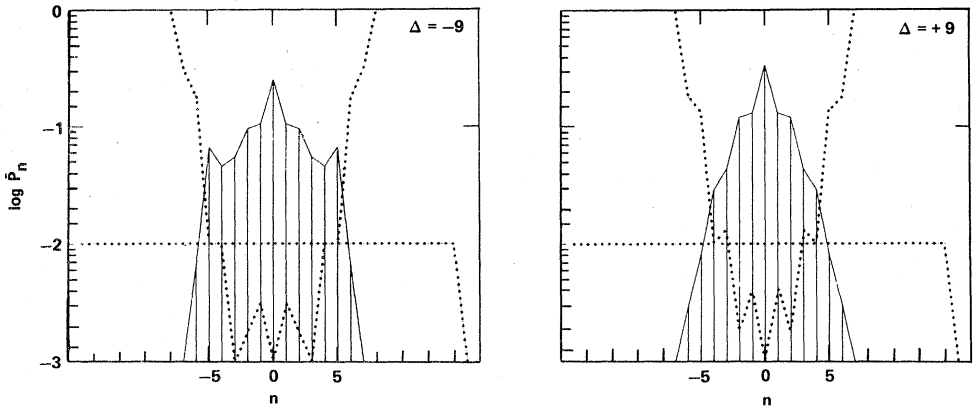

FIG. 8. As in Fig. 6, plots of $\bar{P}_n$ (full lines) and of $|W_{nn}|$ and $|\Omega_n|$ (dotted lines), here for orthogonal laser and atom beams ($q=0$) with $\Omega=16$; (a): $\Delta=-9$, (b): $\Delta=+9$.

integer, we encounter resonance between level $n=0$ and level $n=2q$. It is interesting to note that the condition for this resonance is the Bragg condition: Let $\lambda_A \equiv 2\pi\hbar/p$ be the de Broglie wavelength of the atoms and $d \equiv 2\pi/k$ be the laser wavelength. Then the atomic angle of incidence is

$$\Theta_0 = \arcsin(p_0/p) = \arcsin(q\lambda_A/d), \tag{12.1}$$

and the condition for resonance is that $2q=n$. Thus we obtain the familiar Bragg equation

$$\sin\Theta = n\lambda_A/2d. \tag{12.2}$$

Observe that it is the spacing of the electric-field periodicity d, not the intensity periodicity $d/2$, that determines the Bragg condition.

Note that the probability shifts between the undeviated beam and the Bragg scattered beam and back again; see Fig. 7. This periodic oscillation of probability between level $n=0$ and level $n=2q$ in the N-level model occurs at an effective Rabi frequency Ω_q which one can estimate from the perturbation theory formula[12]

$$\frac{\Omega_q}{2b} = \left(\frac{\Omega}{2b}\right)^{2q} \frac{1}{[(2q-1)!]^2}, \tag{12.3}$$

where $b=\hbar k^2/2M$. Although it would be interesting to observe such spatial manisfestations of Rabi oscillations, the times are too long for practical observation.

XIII. FREQUENCY DETUNING

Because the dynamics of N-level excitation is governed by the balance between diagonal and off-diagonal elements of the RWA Hamiltonian, we can, by inspection of these elements, readily understand the effect of frequency detuning. Whereas the off-diagonal elements remain fixed and independent of n, frequency detuning away from resonance by amount Δ causes successive diagonal elements to become alternatively $+\Delta/2$ and $-\Delta/2$ by taking as zero-point energy the expression

$$E_0 = \frac{1}{2M}(p_1)^2 + \frac{1}{2M}(p_0)^2 - \frac{\hbar\Delta}{2}, \tag{13.1}$$

we obtain diagonal magnitudes having the form

$$f(n) = \begin{cases} |b(2qn+n^2)|, & \text{even } n \\ |b(2qn+n^2)-\Delta|, & \text{odd } n \end{cases} \tag{13.2}$$

A plot of $f(n)$ versus n now reveals a sawtooth pattern imposed upon the previous resonantly tuned pattern. As inspection of Fig. 8 will show, the effect of this sawtooth pattern depends on the sign of the detuning: when $\Delta<0$ probability spreads over a wider range of n values—there is enhanced deflection—whereas when $\Delta>0$ the probability is more confined—smaller deflections.

CONCLUSION

We have analyzed a quantum-mechanical model of deflection of a two-level atom by a standing wave field. Using the analogy with N-level dynamics we have provided an intuitive picture of the deflection process, including effects of angle of incidence and laser frequency.

ACKNOWLEDGMENTS

We have benefited from numerous lengthy discussions of this problem with Dr. R. J. Cook whose insights we gratefully acknowledge. One of us (BWS) wishes to express appreciation for useful conversations at the 2nd International Conference on Multiphoton Processes in Budapest, with Dr. S. Stenholm, Dr. M. V. Fedorov, Dr. J. Bergou, and Dr. S. Varro, each of whom has contributed to the problem of electron deflection by a laser beam. This work was performed under the auspices of the U. S. Department of Energy by the Lawrence Livermore National Laboratory under Contract No. W-7405-ENG-48.

*Present address: Quanta-Ray, Inc.; 1250 Charleston Road, Mountain View, CA 94043.

[1]Cf. the reviews by A. P. Kazantsev, Usp. Fiz. Nauk 124, 113 (1978) [Sov. Phys. Usp. 21, 58 (1978)]; S. Stenholm, Phys. Rep. C43, 151 (1978).

[2]R. J. Cook and A. F. Bernhardt, Phys. Rev. A 18, 2533 (1978).

[3]R. Frisch, Z. Phys. 86, 42 (1933); A. Ashkin, Phys. Rev. Lett. 25, 1321 (1970); A. F. Bernhardt, Appl. Phys. 34, 19 (1976).

[4]R. Schieder, H. Walther, and L. Woste, Opt. Commun. 5, 337 (1972); J. L. Picque and J. L. Vialle, *ibid.* 5, 402 (1972); A. F. Bernhardt, D. E. Duerre, J. R. Simpson, and L. L. Wood, Appl. Phys. Lett. 25, 617 (1974); Opt. Commun. 16, 166 (1976); 16, 169 (1976).

[5]R. J. Cook, Phys. Rev. Lett. 41, 1788 (1978).

[6]C. V. Raman and N. S. N. Nath, Proc. Indian Acad. Sci. 2, 406 (1936); M. V. Berry *The Diffraction of Light by Ultrasound* (Academic, London, 1966).

[7]M. V. Federov, Zh. Eksp. Teor. Fiz. 52, 1434 (1967) [Sov. Phys.—JETP 25, 952 (1967)]; J. K. McIver and M. V. Federov, Zh. Eksp. Teor. Fiz. 76, 1996 (1979) [Sov. Phys.—JETP 49, 1012 (1979)]; M. V. Federov and J. K. McIver, Opt. Commun. 32, 179 (1980).

[8]S. Stenholm, J. Appl. Phys. 15, 287 (1978); S. Stenholm and J. Javanainen, *ibid.* 16, 159 (1978); E. Arimondo, H. Lew, and T. Oka, Phys. Rev. Lett. 43, 753 (1979).

[9]J. T. Haugen, J. Chem. Phys. 65, 1035 (1976); T. H. Einwohner, J. Wong, and J. C. Garrison, Phys. Rev. A 14, 1452 (1976); J. Wong, J. C. Garrison, and T. H. Einwohner, *ibid.* 16, 213 (1977); B. W. Shore and J. Ackerhalt, Phys. Rev. 15, 1640 (1977).

[10]V. S. Letokhov and A. A. Makarov, Opt. Commun. 17, 250 (1976); A. A. Makarov, Zh. Eksp. Teor. Fiz. 72, 1749 (1977) [Sov. Phys.—JETP 45, 918 (1977)]; B. W. Shore and J. H. Eberly, Opt. Commun. 24, 83 (1978).

[11]J. H. Eberly, B. W. Shore, Z. Bialynicka-Birula and I. Bialynicki-Birula, Phys. Rev. A 16, 2038 (1977); Z. Bialynicka-Birula, I. Bialynicki-Birula, J. H. Eberly, and B. W. Shore, *ibid.* 16, 2048 (1977).

[12]W. L. Bragg, Proc. Cambridge Philos. Soc. 17, 43 (1912); W. L. Bragg, Nature (London) 90, 410 (1912); W. L. Bragg and W. L. Bragg, Proc. R. Soc. London 88, 428 (1913); cf. F. K. Richtmyer, E. H. Kennard, and T. Lauritsen, *Introduction to Modern Physics*, 5th ed. (McGraw-Hill, New York, 1955), Chap. 8.

[13]L. Allen, and J. H. Eberly, *Optical Resonance and Two-Level Atoms* (Wiley, New York, 1975).

[14]E. A. Power, *Introductory Quantum Electrodynamics* (Longmans, Green, London, 1964).